ELSEVIER

International Journal of Mass Spectrometry 218 (2002) 75–85

International Journal of Mass Spectrometry

www.elsevier.com/locate/ijms

A novel electron source for negative ion mobility spectrometry

Mahmoud Tabrizchi*, Azra Abedi

College of Chemistry, Isfahan University of Technology, Isfahan 84154, Iran

Received 22 February 2002; received in revised form 9 April 2002; accepted 11 April 2002

Abstract

The possibility of using negative corona discharge in pure nitrogen as the ionization source for negative ion mobility spectrometry (IMS) has been investigated. The discharge in pure nitrogen produces a huge number of electrons, almost 10^6 times as much as that produced by the conventional ^{63}Ni ionization source. However, this high intensity electron source cannot be simply used in IMS since introducing any electronegative substance in the corona region immediately results in quenching of the discharge. In this connection, a special IMS cell has been designed and optimized to employ this intense electron source without being disturbed by sample. With this design, the electron current received at the detector plate could be as high as 200 nA. The ionization efficiency and the collection efficiency of the electrons and negative ions, as a function of electric field at different regions, have been evaluated. As practical examples, the IMS spectra of $CHCl_3$, $CHBr_3$, CH_3I and nitrobenzene, as well as the explosive materials pentaerythritol tetranitrate (PETN) and trinitrotoluene (TNT) at elevated temperatures have been obtained. Finally, the capability of the method in quantitative analysis of $CHCl_3$ has been evaluated and a detection limit of 10 ng/m^3 and a linear range of five orders of magnitude were obtained. (Int J Mass Spectrom 218 (2002) 75–85) © 2002 Elsevier Science B.V. All rights reserved.

Keywords: Ion mobility spectrometry; Negative corona discharge; Chloroform; Nitrobenzene; Trinitrotoluene

1. Introduction

Ion mobility spectrometry (IMS) is a simple, inexpensive and sensitive analytical method for the detection of organic trace compounds [1–4]. The most common ionization source used in IMS is a 12 mCi radioactive ^{63}Ni foil which is advantageous in terms of simplicity, stability and no need for extra power source. However, the radioactivity of ^{63}Ni is disadvantageous in terms of the need for regular leak test and special safety regulations. In addition, the ion generation rate of ^{63}Ni source is not high enough, resulting in weak signals and a low dynamic range. Several other ionization techniques such as, photoionization by ultraviolet light [5], alkali cation emitters [6], surface ionization [7], electrospray [8] and corona discharge [9,10] have been considered as a substitute for the radioactive ^{63}Ni in IMS. In this connection, trace gas analyzers which use UV lamps as the ionization source have been developed by IUT Ltd. [5]. In addition, an IMS cell, applying a corona discharge assembly (with a point-to-ring geometry) as the ion source has been developed and fitted to the Bruker RAID-1 IMS [11]. Furthermore, a pulsed corona discharge ion source, with a point-to-point geometry, for use in analytical instruments and in particular for use in ion mobility spectrometer has been developed [12]. The pulsed corona ion source was employed in a

* Corresponding author. E-mail: m-tabriz@cc.iut.ac.ir

1387-3806/02/$ – see front matter
PII S1387-3806(02)00643-7

lightweight chemical detector, developed by Graseby Dynamics Ltd. [13]. Recently, halogenated hydrocarbons in nitrogen have been determined up to ng/L range with a five order linear range by partial discharge negative ion mobility spectrometry [14]. Partial discharge causes intensive fragmentation of the ions. For example, more than 10 different ions were formed for perfluoro-*n*-pentane after partial discharge ionization [14], resulting in a rather busy and broad spectrum.

A detailed description of design and optimization of a continuous corona discharge ionization source for ion mobility spectrometry is given in our previous work [15]. The reliability of using positive corona discharge and the capability of the method in quantitative analysis have also been demonstrated [16]. The dominant reactant ions produced in the positive corona discharge in air or nitrogen are $(H_2O)_nH^+$ [17]. Then the sample molecules, with proton affinities higher than that of water are easily ionized via proton transfer reaction with the protonated water clusters. However, for the case of negative polarity, when the corona discharge was used in air, nitrogen oxides were produced in the discharge and consequently the ions of the type $NO_x{}^-(H_2O)_n$ were formed [15,18,19]. These ions of very high electron affinity, prevent ionization of other substances, even halogenated compounds. One effective way to eliminate nitrogen oxides is to use a pulsed corona discharge instead of a dc one [9,12,13]. Another possibility is to eliminate oxygen from the discharge region by using pure non-electron attaching gases such as nitrogen or helium. The advantage of using pure nitrogen for negative discharge is to produce a large number of electrons. The electron density in the negative corona discharge in pure nitrogen was found to be about 10^6 times as much as that produced by the ^{63}Ni source [15]. In such a high electron density, electron capture efficiency is very high, thus, the linear range and the sensitivity for detecting electronegative species is expected to be enhanced considerably. Unfortunately, such an intense electron source is quenched when sample is introduced in the ionization region. In this situation, the corona discharge turns off and the electron production is terminated. Our main objective in this work has been the special designing of an IMS cell such that the diffusion of sample into the discharge region is prevented. The optimization of this electron source for negative ion mobility spectrometry and the capability of the method in quantitative analysis, as well as example applications will be described.

2. Experimental

The ion mobility spectrometer used in this study was constructed in our laboratory at the Isfahan University of Technology. A schematic diagram of the spectrometer is shown in Fig. 1. The instrument is very similar to that described previously [15], except for the ionization source that has been slightly modified. The IMS cell is a glass tube, 4 cm inner diameter and 19 cm long, on which 15 stainless steel guard rings are mounted. The guard rings are located 1 mm apart from each other and connected by a series of resistors to form the electric field. The corona electrode is a thin gold wire (0.05 mm diameter), supported by a needle, which is inserted in a Teflon piece, fixed at one end of the glass tube. In order to limit the discharge current, a 5 MΩ protective resistor was used in series with the discharge. The target electrode was made of a 2-mm thick graphite disc with a hole (1.5 mm diameter) at the center, mounted and sealed inside the glass tube in front of the needle to create a point-to-plane geometry. Another graphite disc called the *curtain electrod*e, with the same size as the target electrode, was mounted in parallel to and at 9 mm distance from the first disc. A flow of dry nitrogen (about 150 mL/min) was introduced between the two discs and exited from the both holes. This gas served as a curtain and separated the discharge region from the ionization region, where the sample was introduced. In fact, the curtain gas prevented the diffusion of the sample into the corona region and the diffusion of neutral corona products into the ionization region. The detailed description of the gas flow directions is given in Fig. 2. Three homemade high-voltage power supplies were employed in this work and connected to the electrodes as illustrated in

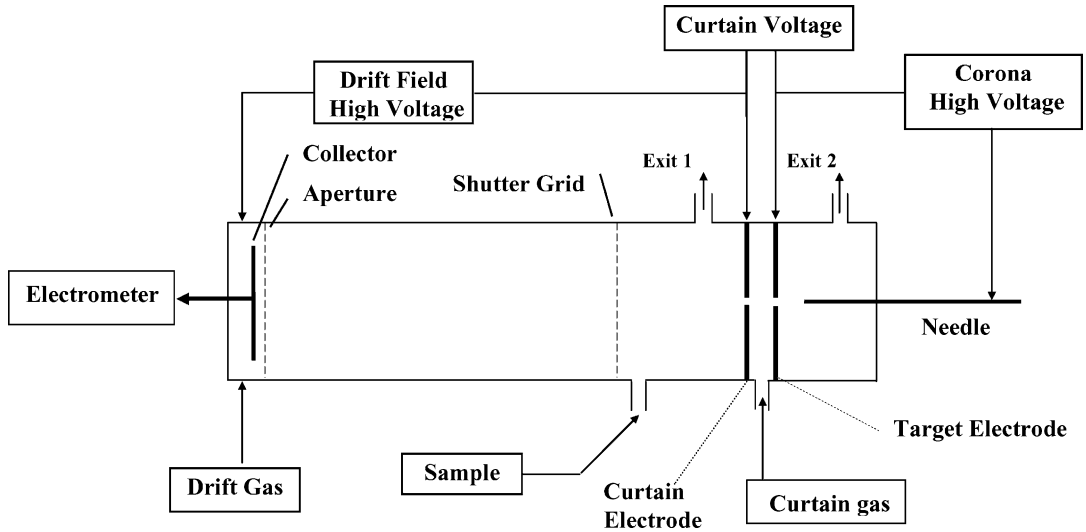

Fig. 1. Schematic diagram of negative corona discharge IMS.

Fig. 1. A single 10,000 V power supply for creating the drift field, an isolated one (5000 V) for the corona discharge and a second isolated power supply for applying a voltage (300–2500 V) between the two discs to pull electrons through the target electrode towards the curtain electrode. The distance between the shutter grid and the curtain electrode was 4 cm and the drift length was 11 cm. The electric field strength in the drift region and the ionization region varied between 350 and 630 V/cm. The ion current was amplified by an electrometer with a gain of 10^7 or 10^8 V/A (as required) and after further amplification was fed to the

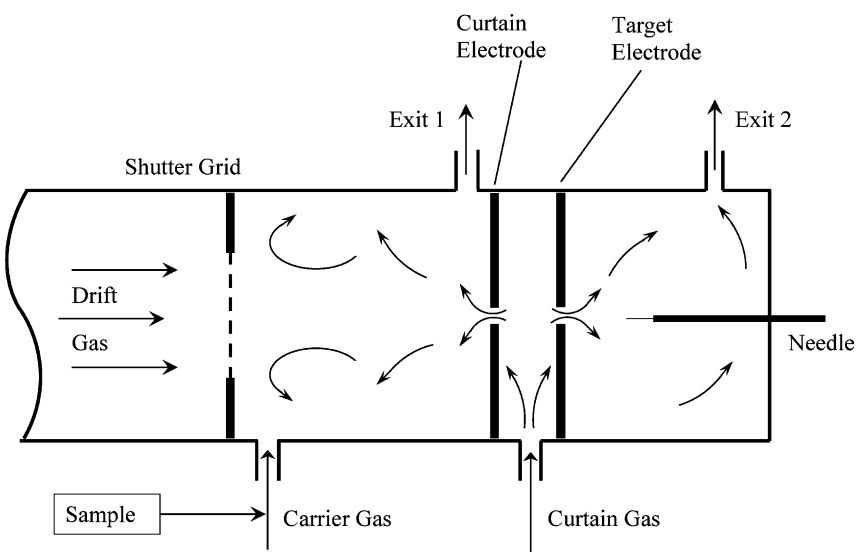

Fig. 2. Detailed description diagram of the negative corona discharge source showing the corona needle, the target electrode, the curtain electrode and the gas flow directions.

computer via an A/D converter. The digitized signal-could be averaged over a number of scans, and the resulting ion mobility spectrum was displayed on the monitor. Typically, a 100 μs pulse for shutter grid was used during the measurements.

The gas used in this work was pure nitrogen (99.9995%, Internmar B.V., The Netherlands). Water vapor and other contaminations were removed by passing the gas through a 13× molecular sieves (Fluka) trap before entering the IMS. The flow rates of the carrier, the curtain and the drift gases were about 100, 150 and 600 mL/min, respectively.

3. Results and discussions

3.1. The negative corona discharge

The negative discharge in nitrogen was first investigated by monitoring the electrical current passing through the needle while the dry nitrogen was flowing with a flow rate of approximately 600 mL/min. As the potential of the needle was increased, around 1.2 kV, a current in the order of a fraction of mA was observed. The threshold of the discharge was dependent on the needle-to-plane distance and was considerably lower than that of the positive polarity for the same distance. The discharge was localized on the point tip with a bright violet glow spot, wandering randomly on the point tip. This wandering causes the discharge current to fluctuate. The introduction of the smallest amount of oxygen or any electron attaching substance into the discharge region immediately caused the current to drop to nearly zero.

The discharge current for negative corona was much higher than that observed for the positive corona, which is usually in μA range under the same conditions [15]. The high current observed for the negative corona in pure nitrogen can be explained considering the mechanism of the negative corona discharge [20,21]. In a point-to-plane geometry, the electric field is very strong in the vicinity of the tip. At a sufficient voltage, electrons leaving the negative point are multiplied due to electron impact ionization of the gas molecules. Positive ions hitting the negative tip knock out more electrons and ensure the reproduction of electrons removed by the field. Since no negative ions are formed in nitrogen, the positive ions are accelerated in the high field region towards the point without interruption by negative space charges. The positive ions hit the point surface with energies 10–100 times higher than the energies with which they would strike the negative plate during a positive corona [22]. Therefore, the current for the negative corona discharge in pure nitrogen, or any non-electron attaching gas such as helium, argon or hydrogen, is expected to be much higher than that of the positive corona. It is also well known that the metastable $N_2(A^3\Sigma_u^+)$ molecules are involved in negative corona discharge in pure nitrogen [23]. The metastable molecules are produced following the electron impact on the nitrogen molecules. These excited molecules release electrons from the tip during the collision with its surface. The photoelectric effect also causes electron emission from the cathode. At low pressure, ion bombardment is the dominant process but at atmospheric pressure the most probable process for electron emission from the cathode is the metastable molecule impact on the surface [23–25].

The work function of the point and its condition would greatly influence the electron emission. The continuous bombardment of the needle electrode alters its work function and consequently the discharge is affected. This may explain the movement of the concentrated discharge over the surface [22]. Application of a thin gold wire as the tip stabilized the discharge and gave a constant current. This is probably due to the higher efficiency of electron emission by metastable molecule bombardment for the case of gold [23].

Introducing electron-attaching substances, results in the formation of negative ions via electron capture process. The negative ions move much slower than the electrons and remain in the vicinity of the tip. The negative ion space charge cloud interrupts the positive ion bombardment and acts to choke off the discharge [22]. Impurities also extinguish the metastable states effectively, so that the medium near the point layer is changed. Consequently, in the presence of impurity,

the discharge current decreases and at a sufficient concentration the discharge turns off [24].

In order to evaluate the effect of voltage on the discharge, the current, I, was measured as a function of the needle voltage, V, at different needle-to-plane distances. Unlike the positive corona, a plot of I/V vs. V is not a straight line. This is inconsistent with the characteristics of low current self-sustained coronas where I/V is a linear function of V [20]. However, as demonstrated in Fig. 3, the current is a linear function of the potential. In general, the current is proportional to $(V - V_0)$, where V_0 is the ignition potential. If the Ohm's law is applied here, the slope of the I–V plot is the reciprocal of the resistance. Considering the 5 MΩ protective resistor in series with the discharge, the electrical resistance of the discharge can be calculated from the slopes in Fig. 3. For a 5 mm needle-to-plane distance, the discharge resistance is about 0.9 MΩ and it was found to be generally related to the distance by $R(\mathrm{M\Omega}) = 0.18d$ (mm). The ignition potential, V_0, can also be obtained from the intercept of the I–V plots. The results show that the ignition potential, V_0, is a linear function ($r^2 = 0.989$) of the discharge gap length by V_0 (kV) $= 0.83 + 0.10d$ (mm). The discharge current was also measured at various temperatures. The current increased by almost 16% when the temperature increased from room temperature up to 250 °C.

3.2. Collection of electrons

The total current reaching the collector plate was measured while the shutter grid left totally open.

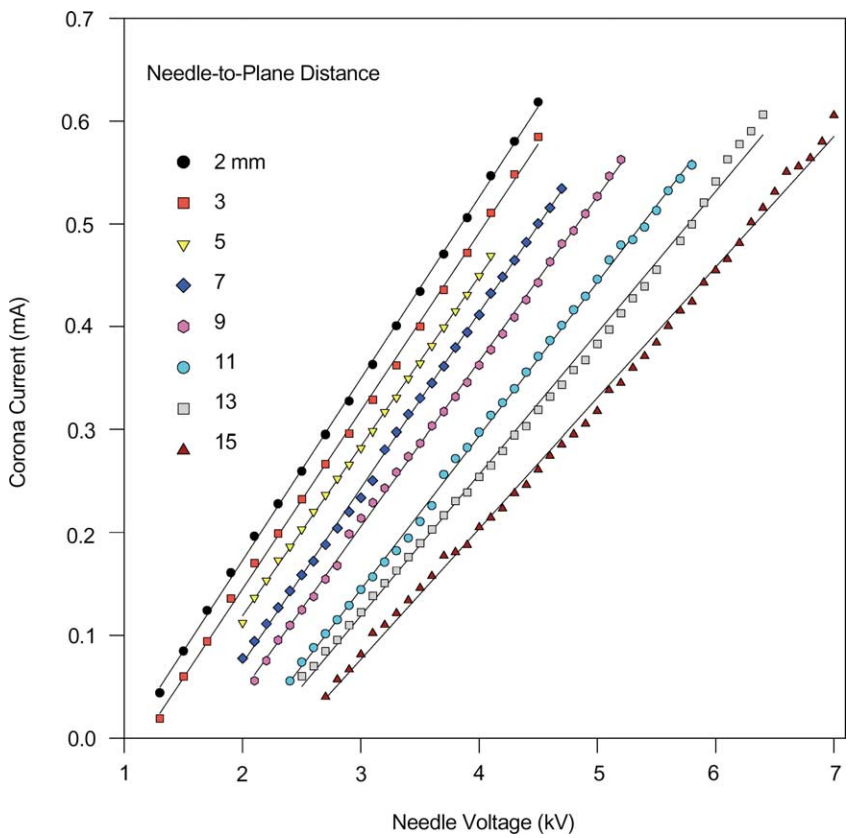

Fig. 3. The plot of the discharge current vs. needle voltage at several fixed needle-to-plane distances.

The current was found to be only about 0.1% of the discharge current. The large reduction in electron current is partly due to the small hole-size in the two graphite discs that let only a portion of electrons to pass. In addition, the electric field in both sides of the first disc differs very much. The ion transmittance from the target electrode, with a grid instead of a disc, was found to be about the ratio of E_2/E_1, where E_2 and E_1 are the electric fields after and before the counter electrode, respectively [15]. At operating conditions the ratio E_2/E_1 is usually small so that a small percentage of the electrons are expected to pass the first disc. The second disc also reduces the number of electrons. In conclusion, the electron transmittance from this configuration is less than the ion transmittance from the positive corona in the previous work [15]. However, due to the high discharge current, the electron current received at the collector plate could be as high as 200 nA.

The total electron current received on the collector plate was not very sensitive to the needle voltage but it was strongly dependent on the drift field and the voltage between the two discs. Fig. 4 shows the collector current vs. the drift field at different voltages applied between the two discs. In general, the electron current increases by both the drift field and the curtain voltage. For the case of the positive corona discharge, it was shown that the collection efficiency of the drift tube is a quadratic function of the electric field [15]. Similarly, the electron current starts rising quadratically but the curves change their slope to approach a plateau. It seems that, at high drift fields, the voltage between the two discs determines the electron transmittance. The effect of the curtain voltage on collecting the electrons at constant drift fields can also be seen in Fig. 4. The collected current increases almost linearly by increasing the curtain voltage but again it reaches a certain level. The curves in Fig. 4 fit

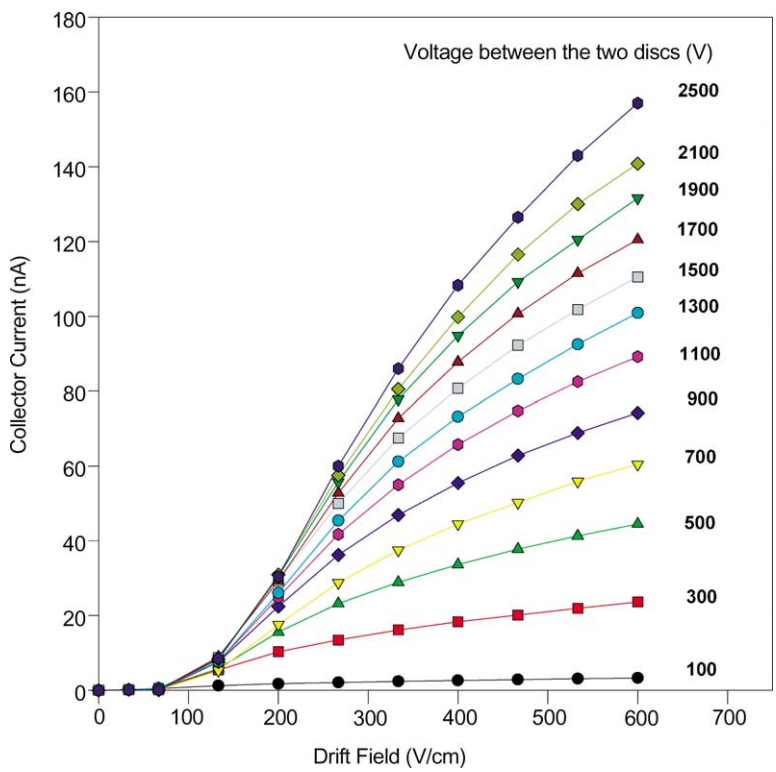

Fig. 4. The total current received at the collector plate as a function of the drift field at several voltages applied between the target and the curtain electrodes.

reasonably well in a function of the form:

$$\frac{1}{I} = \frac{a}{E_d^2} + \frac{b}{E_c}$$

where a and b are constants and E_d and E_c are the drift and the curtain fields, respectively. Since the ion transmission for the drift tube is proportional to the square root of the drift field [15], the term a/E_d^2 may be interpreted as the ionic resistance for the drift tube. The term b/E_c may also be assumed as the ionic resistance for the curtain. Then the reciprocal of the current ($1/I$), which represents the total resistance, would be the sum of the two resistors.

3.3. The background spectrum

The background ion mobility spectrum of pure nitrogen is shown in Fig. 5. The spectrum shows a very large peak at zero drift time corresponding to electrons, and two small peaks corresponding to negative ions. When oxygen was injected to the carrier gas, the second negative ion peak was increased. Accordingly, the origin of the negative ions was thought to be due to the presence of trace amounts of oxygen in the gas. Although the nitrogen used in this experiment was highly pure, it may contain about 5 ppm oxygen, which seems to be enough for the production of negative ions in such an intense electron source. Another source of oxygen could be the diffusion of ambient air into the IMS cell, although careful attempts were made to seal all the joints and connections. Nitrogen oxides may also be formed in the discharge at trace levels. This is possibly the source of appearing the first negative ion peak. Despite the presence of negative ions, their total intensity is negligible with respect to that of electrons. The electrons/negative ions ratio was dependent on the curtain voltage and the drift field as well as the purity of the nitrogen gas. The observed ratio could be at most close to 40.

3.4. The curtain gas

The ratio of electrons to the negative ions was also sensitive to the flow rate and the flowing direction of the curtain gas. When the curtain gas entered from exit 2 (shown in Fig. 2), the ratio of electrons to the negative ions was decreased considerably. In addition, more peaks appeared and the first negative ion peak increased while the oxygen peak decreased. The corresponding spectra are inserted in Fig. 5. The decreasing of the oxygen peak reveals that a species with very high electron affinity is present in the ionization region. Nitrogen oxides, formed in the corona discharge, are the possible candidates. When the curtain gas is entering from exit 2, the gas and electrons in front of the needle are moving in the same direction, towards the ionization region. Thus, the discharge products, such as nitrogen oxides, are carried out to the ionization region and convert electrons to negative ions. This could be the reason for reducing the ratio of electrons to the negative ions and the appearing of more peaks in the spectrum. In order to maximize the electron production and minimize the background negative ions, the curtain gas was chosen to flow towards the needle tip, opposite to the direction of the electrons, as shown in Fig. 2. The opposite force arising from the countercurrent stream of the curtain gas on the negative ions is not considerable. However, the curtain gas prevents the diffusion of neutral corona products into the ionization region. It also keeps the discharge region free from sample. The injection of the sample into the carrier gas did not affect the discharge at all. This was confirmed by monitoring the discharge current while the sample was injected. Negative ion mobility spectra of several test compounds, $CHCl_3$, $CHBr_3$, CH_3I, nitrobenzene and the explosive materials, pentaerythritol tetranitrate (PETN) and 2,4,6-trinitrotoluene (TNT) are presented in Fig. 6. The peak appearing in the $CHCl_3$ spectrum probably corresponds to the hydrated Cl^- ion since a peak at the same drift time was observed when other chlorinated compounds such as CCl_4 or chlorobenzene were injected. Similarly the peaks appeared in the $CHBr_3$ and CH_3I spectra may also correspond to the hydrated Br^- and I^- ions, respectively. Halogenated compounds normally produce halide ions via a dissociative electron capture reaction. The reduced mobilities measured for the major peaks in the spectra of $CHCl_3$, CH_3Br and CH_3I are in good agreement with

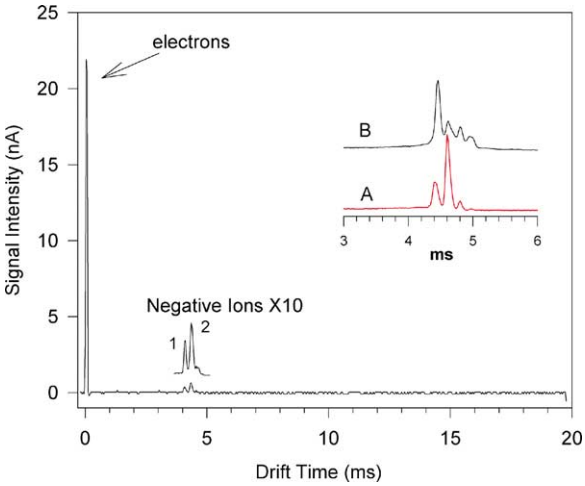

Fig. 5. Background negative ion mobility spectrum of pure nitrogen recorded with negative corona discharge ionization source. Spectrum A is recorded when the curtain gas is flowing opposite to the needle as shown in Fig. 2 while for spectrum B the curtain gas is entering from the exit 2 and carrying the corona products into the ionization region.

the reported values; 2.92, 2.63 and 2.53 $cm^2/V\,s$ for Cl^-, Br^- and I^- ions, respectively [26].

The general shape of the PETN spectrum is similar to that recorded with ^{63}Ni ionization source [27] but with a better resolution and a higher signal to noise ratio. Mass spectrometry investigation of PETN with thermal electrons shows that there are complex ionic species with the largest one being $PETN{\cdot}NO_3^-$ ion and a significant amount of NO_3^- ions [28]. The reduced mobility value for the first PETN peak is very close to the reduced mobility of NO_3^- (2.46 $cm^2/V\,s$) reported by Ewing et al. [29]. Therefore, the first and the last peaks in the PETN spectrum might be originated from NO_3^- and $PETN{\cdot}NO_3^-$ ions. The TNT and nitrobenzene spectra show only one peak with reduced mobilities of 1.55 and 1.86 $cm^2/V\,s$, respectively. These values are close to the reported values by Spangler and Lawless [30] for TNT^- (1.49) and $C_6H_5NO_2^-$ (1.87). Unlike halogenated compounds nitrotoluenes and nitrobenzene capture electrons nondissociatively and produce M^- in the absence of a proton abstracting agent [30].

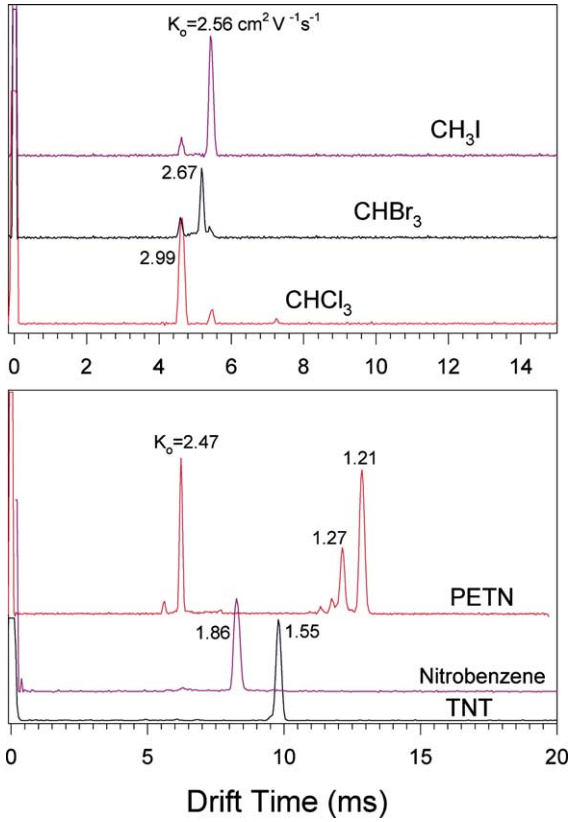

Fig. 6. Negative ion mobility spectra of $CHCl_3$, $CHBr_3$, CH_3I, nitrobenzene and the explosives, PETN and TNT recorded with negative corona discharge ionization source at 160 °C.

3.5. Ionization efficiency and ion collection

Sample molecules are ionized in the ionization region via electron attachment. The ionization region is the gap between the curtain electrode and the shutter grid. It was found that if the sample concentration is increased up to a level that all electrons are consumed, the negative ion intensity is not as high as the original electron intensity. The reduction could be due to the fact that the collection efficiency for fast moving electrons is higher than that of the ions which move relatively slower.

The collection efficiency was also dependent on the electric field in the ionization region. An increase in the electric field results in a higher ion collection.

On the other hand, the residence time of electrons in the ionization region decreases if the field is increased, i.e. the higher the ionization field is, the less time for electrons to be captured. Therefore, at high fields the ion generation rate is low but the ion collection efficiency is high and at low ionization fields the reverse trend is true. In conclusion, the ion intensity is expected not to be very sensitive to the ionization field. In order to examine this, a fourth-isolated power supply was employed to independently vary the voltage between the curtain electrode and the ring before the shutter grid. A constant flow of chloroform vapor, in ppb ranges, was injected into the carrier gas. Under this condition, the negative ion signal was monitored while the voltage varied. It was noticed that, the Cl^- ion intensity was almost constant at various ionization fields, within the range of 13–330 V/cm, i.e. the ion intensity was not sensitive to the ionization field, as expected.

Unlike negative ions, the electron intensity was strongly under influence of the ionization field. The electron intensity as a function of the ionization field is shown in Fig. 7. It increases by more than three times when the field changes from 13 to 530 V/cm. This is because more electrons are extracted from the curtain gap at higher electric fields. If the sample concentration is increased up to the saturation level, where all electrons are converted to negative ions, the ion intensity becomes also field dependent. This is demonstrated in Fig. 7 where the Cl^- ion intensity has been multiplied by a factor of 3. At high sample concentrations, the residence time of electrons is not important since all electrons, regardless of their speed, are captured at the beginning of the ionization region. In this situation, the number of negative ions produced in the ionization region is proportional to the number of electrons entering that region which itself is field-dependent. Therefore, at high concentrations, the negative ion intensity increases with the ionization field. The general conclusion is that, high ionization fields give a better sensitivity at high concentrations but it has no effect on the sensitivity at low concentrations. The ionization field in this work was chosen as high as the drift field [13].

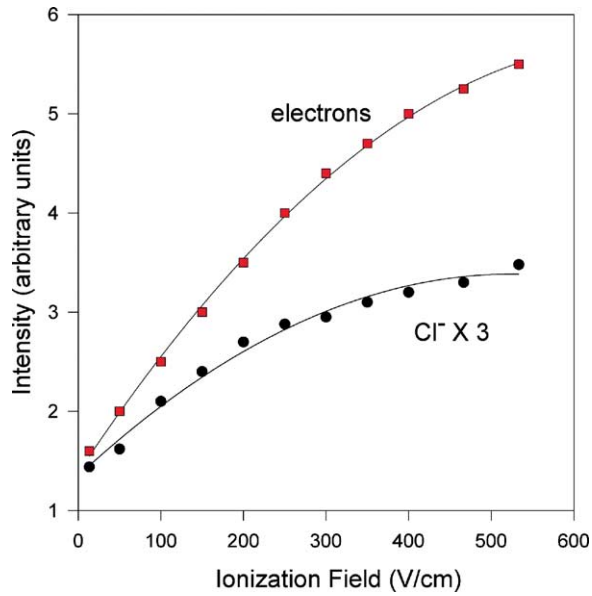

Fig. 7. The electron and the Cl^- ion intensities as a function of the electric field between the curtain electrode and the shutter grid. The drift field and the curtain voltage are 363 V/cm and 1000 V, respectively. The discharge voltage was 1.5 kV and the gap was 4 mm.

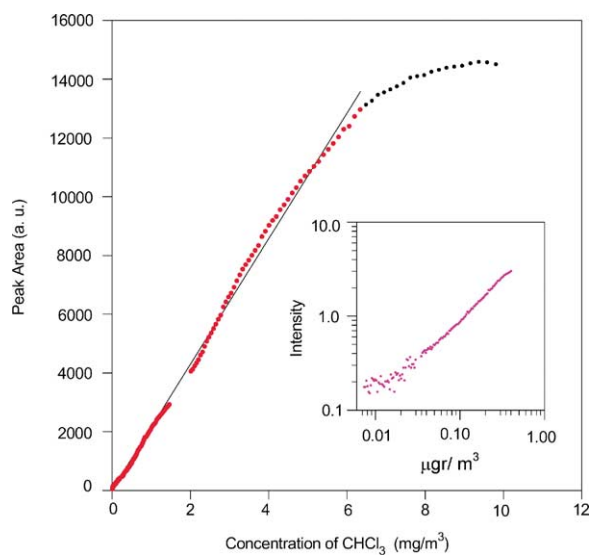

Fig. 8. The area under the Cl^- ion peak vs. the chloroform concentration.

3.6. The linear and the working range

The application of IMS for quantitative analysis is limited because of its restricted linear range and its narrow working range. The proposed solution is to use a servo-inlet [31,32] in which the sample is pulsed with a fast valve into the inlet against a flow of clean air or nitrogen [2]. The air/sample ratio is adjusted so that the reactant ion peak intensity stays within a preset range.

Commonly, linear ranges of 10–100 have been reported for the conventional IMS using ^{63}Ni ionization source [2]. The working range can hardly be near or above 1000. The main reason for such short linear and working ranges is the limited amounts of ions generated by the ^{63}Ni source. The total ion current of a 12 mCi ^{63}Ni ionization source is below 1 nA [6]. However, the total electron current in the negative corona discharge in pure nitrogen is about a fraction of mA. If only 1/1000 of this large number of electrons enter the ionization region, then the electron density is still larger than that of ^{63}Ni by at least two orders of magnitude. Such an increase in the electron density will certainly results in a larger linear range and wider working range. In order to evaluate the linear range, the exponential dilution flask method was used to introduce the sample. This technique is well known for introducing gas samples into IMS [30]. In this method, a known amount of sample is introduced into a vessel. Then, the vessel is continuously flushed out with a carrier gas. The outlet analyte concentration (C) after time (t) is given by $C = C_0 \exp(-Qt/V)$, where C_0 is the initial concentration of the analyte, Q the gas flow rate and V is the vessel volume. A stock chloroform standard sample was prepared by injecting 10 μL of chloroform saturated headspace gas at 26 °C, into a calibrated 331 mL volume flask via a gas tight syringe. Considering the vapor pressure of chloroform at 26 °C, which is 199 mmHg, the initial chloroform concentration in the flask would be 38 mg/m^3. The flask was flushed with the carrier gas at a flow rate of 244 mL/min and its outlet was directly connected to the IMS cell. Two hundred and fifty spectra were averaged every 5 s for 10 min. Then the area under the Cl^- ion peak at different dilution times was measured. Fig. 8 shows the observed ion signal vs. the calculated chloroform concentration based on the dilution flask equation. The missing points correspond to the time when the amplifier was saturated and its gain needed to be changed. In order to accurately measure the signal at low concentrations, the experiment was repeated at higher sensitivity with a 3.8 μg/m^3 initial concentration. The results are demonstrated in log–log scale and inserted in Fig. 8. The linear and the working range have been extended dramatically. The dynamic range ($R = 0.995$) is more than five orders of magnitude and the detection limit is below 10 ng/m^3. Such linear range and sensitivity in negative corona discharge ion mobility spectrometry can be compared to those obtained after partial discharge ion mobility spectrometry [14]. The long linear range is due to the very high initial electron density, produced by the corona discharge.

3.7. Conclusions

There are two problems associated with the use of continuous negative corona discharge in IMS. The first is the production of NO_x in the discharge. Nitrogen oxides with very high electron affinities do not allow other compounds to form negative ions. If pure nitrogen is used to prevent NO_x production, then the second problem appears, i.e. the discharge turns off when sample is injected. In this work, it was shown that ion mobility spectrometers could be equipped with negative corona discharge as the ionization source without interference of NO_x or disturbance of the discharge by sample. This was achieved by use of pure nitrogen in the discharge region and employing a curtain gas to separate the discharge region from the ionization region. The advantage of using such ionization source is to boost the electron current up to as high as 200 nA which is larger than that of ^{63}Ni by two orders of magnitude. As a result the detection limit of electronegative substances reduces considerably. This is especially suitable for sensitive detection of explosives and halogenated hydrocarbons. In addition, the use of the high electron density expands the working and the linear range of IMS.

Analysis of mixtures by negative IMS in some cases may also be improved if such intense electron source is used. Electron affinity plays the major role in ionization of samples in negative mode. Different compounds in a mixture compete with each other to capture electrons. At high electron density and low concentrations, enough electrons are available for all compounds in a mixture and the matrix effect may be reduced. However, in the case of halogenated compounds, where the compounds contain the same halogen, a preseparation technique such as gas chromatography is required for analysis of the mixture.

In portable instruments, since only the curtain gas is needed to be pure nitrogen, a small nitrogen or helium source can provide the curtain gas for a time comparable to the battery lifetime. Thus, the portable IMS instruments could be equipped with this ionization source to improve their performance.

Acknowledgements

This research was supported by Grant no. NRCI13 of National Research Projects and with the support of National Research Council of Islamic Republic of Iran. Authors would like to thank M.T. Jafari and I. Ebadi for their help in this work as well as Dr. T. Khayamian and Prof. M. Amirnasr for valuable discussions. This work was presented in part at the 10th International Conference on Ion Mobility Spectrometry, Wernigeroade, Germany, August 2001.

References

[1] T.W. Carr, Plasma Chromatography, Plenum Press, New York, 1984.
[2] G.A. Eiceman, Z. Karpas, Ion Mobility Spectrometry, CRC Press, Boca Raton, 1993.
[3] G.A. Eiceman, Crit. Rev. Anal. Chem. 22 (1991) 17.
[4] R.H. St. Louis, H.H. Hill Jr., Crit. Rev. Anal. Chem. M21 (1990) 321.
[5] J.W. Leonhardt, W. Rohrbeck, H. Bensch, Int. J. Ion Mobility Spectrom. 3 (1) (2000) 43.
[6] K.N. Vora, D.N. Cambell, R.C. Davis, G.E. Spangler, J.A. Reategni, European Patent Appl. EP 198154 AZ (22 October 1986).
[7] U.Kh. Rasulev, Int. J. Ion Mobility Spectrom. 4 (2) (2001) 13.
[8] W.E. Steiner, B.H. Clowers, K. Fuhrer, M. Gonin, L.M. Matz, W.F. Siems, A.J. Schultz, H.H. Hill Jr., Rapid Commun. Mass Spectrom. 15 (2001) 2221.
[9] J. Stach, J. Adler, M. Brodacki, H.R. Döring, in: Proceedings of the Third International Workshop on Ion Mobility Spectrometry, 1995, p. 71.
[10] H. Borsdorf, H. Schelhorn, J. Flachowsky, H.R. Döring, J. Stach, Anal. Chim. Acta 403 (2000) 235.
[11] J. Adler, G. Arnold, H.R. Döring, V. Starrock, E. Wülfing, in: Proceedings of the 6th International Workshop on Ion Mobility Spectrometry, 1998, p. 109.
[12] R. Turner, S.J. Taylor, A. Clark, P.D. Arnold, European Patent, WO9728444 (7 August 1997).
[13] Newsletter of the International Society for Ion Mobility Spectrometry 1 (1998) 13.
[14] H. Schmidt, J.I. Baumbach, S. Sielemann, M. Wember, D. Klockow, Int. J. Ion Mobility Spectrom. 4 (2001) 39.
[15] M. Tabrizchi, T. Khayamian, N. Taj, Rev. Sci. Instrum. 71 (2000) 2321.
[16] T. Khayamian, M. Tabrizchi, N. Taj, Fresenius J. Anal. Chem. 370 (2001) 1114.
[17] M. Pavlik, J.D. Skanly, Rapid Commun. Mass Spectrom. 11 (1997) 1757.
[18] C.J. Proctor, J.F.J. Todd, Org. Mass Spectrom. 18 (1983) 509.
[19] S. Sakata, T.J. Okada, Aerosol Sci. 25 (1994) 879.
[20] J.M. Meek, J.D. Craggs, Electrical Breakdown of Gases, Wiley, Chichester, 1978.
[21] Yu.P. Raizer, Gas Discharge Physics, Springer, Berlin, 1991.
[22] G.L. Weissler, Phys. Rev. 63 (1943) 96.
[23] S.C. Haydon, O.M. Wiliams, J. Phys. B: Atomic Mol. Phys. 6 (1973) 227.
[24] H. Koge, K. Kudu, M. Laan, in: Third International Symposium on High Voltage Engineering, Milan, 28–31 August 1979.
[25] H. Koge, Investigation of Negative Point Discharge in Pure Nitrogen at Atmospheric Pressure, Dissertations, Physica Universitatis Tartuensis, Tartu, Estonia, 1992.
[26] F.W. Karasek, H.H. Hill Jr., S.H. Kim, J. Chromatogr. 135 (1977) 329.
[27] J.P. Davies, L.G. Blackwood, S.G. Davis, L.D. Goodrich, R.A. Larson, Anal. Chem. 65 (1993) 3004.
[28] G.A. Eiceman, D. Preston, G. Tiano, J. Rodriguez, J.E. Parmeter, Talanta 45 (1997) 57.
[29] R.G. Ewing, D.A. Atkinson, G.A. Eiceman, G.J. Ewing, Talanta 54 (2001) 515.
[30] G.E. Spangler, P.A. Lawless, Anal. Chem. 50 (1978) 884.
[31] S.P. Cram, S.N. Chesler, J. Chromatogr. 99 (1974) 267.
[32] W.C. Blanchard, A.T. Bacon, US Patent 4,797,554 (1989).